Near-Infrared Electrochromic Poly(aryl ether)s Based on Isolated Electroactive Tetraphenyl-*p*-Phenylenediamine Moieties

GUEY-SHENG LIOU,[1] HUNG-JU YEN,[1] MING-CHE CHIANG[2]

[1]Functional Polymeric Materials Laboratory, Institute of Polymer Science and Engineering, National Taiwan University, 1 Roosevelt Road, 4th Sec., Taipei 10617, Taiwan

[2]Department of Applied Chemistry, National Chi Nan University, 1 University Road, Puli, Nantou Hsien 54561, Taiwan

Received 3 June 2009; accepted 19 June 2009
DOI: 10.1002/pola.23587
Published online in Wiley InterScience (www.interscience.wiley.com).

ABSTRACT: A series of near-infrared (NIR) electrochromic aromatic poly(aryl ether)s containing *N,N,N′,N′*-tetraphenyl-*p*-phenylenediamine (TPPA) moieties in the backbone were prepared from the high-temperature polycondensation reactions of a biphenol monomer, 2,5-bis(diphenylamino)hydroquinone, with difluoro compounds. The obtained polymers were readily soluble in many organic solvents and showed useful levels of thermal stability associated with high glass-transition temperatures (182–205 °C) and high char yields (higher than 40% at 800 °C in nitrogen). The polymer films showed reversible electrochemical oxidation with high contrast ratio both in the visible range and NIR region, and also exhibited high coloration efficiency (CE), low switching time, and stability for electrochromic operation. The polyether **TPPA-a** thin film revealed good CE in visible (CE = 217 cm^2/C) and NIR (CE = 192 cm^2/C) region with reversible electroactive stability (over 500 times within 5% loss relative to its initial injected charge). © 2009 Wiley Periodicals, Inc. J Polym Sci Part A: Polym Chem 47: 5378–5385, 2009

Keywords: electrochemistry; functionalization of polymers; high performance polymers; poly(ether ketones)

INTRODUCTION

Electrochromic materials exhibit a reversible optical change in absorption or transmittance upon electrochemically oxidized or reduced, such as transition-metal oxides, inorganic coordination complexes, organic molecules, and conjugated polymers.[1] Traditionally, investigation of electrochromic materials has been directed toward optical changes in the visible region (e.g., 400–800 nm), proved especially useful of variable reflectance mirrors, tunable windows, and electrochromic displays. Increasingly, attention of the optical changes has been focused extending from the near infrared (NIR; e.g., 800–2000 nm) through the microwave regions of the spectrum,[2] which could be exploitable for environmental control (heat gain or loss) in buildings. Recently, NIR electrochromic materials such as transition metal oxides (WO3), quinone-containing organic materials, and organic metal complex (ruthenium dendrimer) have been investigated.[3] For organic materials, in addition to conjugated polymers,[4] *N,N,N′,N′*-tetraphenyl-*p*-phenylenediamine (TPPA) containing molecule is a interesting anodic electrochromic system for NIR applications because of its

Correspondence to: G.-S. Liou (E-mail: gsliou@ntu.edu.tw)
Journal of Polymer Science: Part A: Polymer Chemistry, Vol. 47, 5378–5385 (2009)

particular intramolecular electron transfer (ET) in the oxidized states.

Intramolecular ET processes were studied extensively in the mixed-valence (MV) systems,[5] and usually employed one-dimensional MV compounds containing two or more redox states. According to Robin and Day,[6] the TPPA cation radical has been reported as a symmetrical delocalized class III structure with a strong electronic coupling (the electron is delocalized over the two redox centers), leading an intervalence charge transfer (IV-CT) absorption band in the NIR region.[7]

To be useful for electrochromic applications, some key issues such as long-term stability, rapid redox switching, high coloration efficiency (CE), and high optical transmittance change ($\Delta\%T$) during operation played important roles and required to be achieved. In our ongoing effort to develop electrochromic polymeric materials, we have synthesized and investigated a series of triphenylamine (TPA) containing high-performance polymers,[8] which showed good electrochromic reversibility in the visible region. Additionally, we also prepared the analogous polymers bearing pendent variety moieties, and showed observable contrast ratio.[9] Furthermore, our research goal and strategy was extended to prepare the novel TPPA-based electrochromic polymers with absorption band in the NIR region by using conventional polycondensation methods. Because of the incorporation of packing-disruptive TPPA units into the polymer backbone, most of the thermal stable polymers exhibited good solubility in polar organic solvents, thus transparent and amorphous thin films could be prepared by solution casting or spin-coating techniques which are beneficial for their fabrication of large-area, thin-film electrochromic devices.

In this contribution, we therefore synthesized the TPPA-based aromatic polyethers from the diphenol monomer 2,5-bis(diphenylamino)hydroquinone (**TPPA-2OH**) with difluoro compounds. Incorporation of preformed TPA units into poly(aryl ether)s allows the retention of some of the favorable properties of polymers such as high thermal stability and glass transition temperature, whereas the aryl ether linkages increase the solubility and enhance the film-forming ability, facilitating both processing and application.[10] We anticipate that the obtained electrochromic polyethers could reveal quick optical response times with high optical density changes in NIR region. In addition to the general properties (such as inherent viscosities, molecular weights, solubility, and thermal properties), the electrochemical and electrochromic behaviors of these polymers were also investigated.

EXPERIMENTAL

Materials

2,5-Bis(diphenylamino)-1,4-dihydroxybenzene[11] (**TPPA-2OH**) (mp: 204–207 °C) and 2,5-bis(4-fluorophenyl)-1,3,4-oxadiazole[12] (**BF-b**) (mp: 205–206 °C) were synthesized according to a previously reported procedure. 4,4′-Difluoro-benzophenone (**BF-a**) (ACROS) was purified by recrystallization. Tetrabutylammonium perchlorate (TBAP) (ACROS) was recrystallized twice from ethyl acetate under a nitrogen atmosphere and then dried *in vacuo* prior to use. All other reagents were used as received from commercial sources.

Polymer Synthesis

The synthesis of polyether **TPPA-b** was used as an example to illustrate the general synthetic route used to produce the polyethers. To a two necked 50 mL glass reactor was charged with **TPPA-2OH** (0.89 g, 2 mmol), **BF-b** (0.52 g, 2 mmol), and 4 mL *N*-methyl-2-pyrrolidinone (NMP), 2 mL of toluene, and an excess of potassium carbonate (0.42 g, 3 mmol). The reaction mixture was heated at 150 °C for 3 h as dehydration, then heated at 170 °C for 1 h, 180 °C for 3 h, and finally heated at 190 °C for 1 h. After the reaction, the obtained polymer solution was poured slowly into 400 mL of acidified methanol/water (v/v = 1/1). The precipitate was collected by filtration, washed thoroughly with hot water and methanol, and dried under vacuum at 100 °C. Reprecipitations of the polymer by NMP/methanol were carried out twice for further purification. The inherent viscosity and weight-average molecular weights (M_w) of the obtained polyether **TPPA-b** was 0.42 dL/g (measured at a concentration of 0.5 g/dL in NMP at 30 °C) and 25,000, respectively. Anal. Calcd (%) for $(C_{30}H_{24}N_2O_2)_n$ $(444.58)_n$: C, 79.50; H, 4.85; N, 8.43. Found: C, 80.44; H, 5.16; N, 8.06. The other polyether **TPPA-a** was prepared by an analogous procedure.

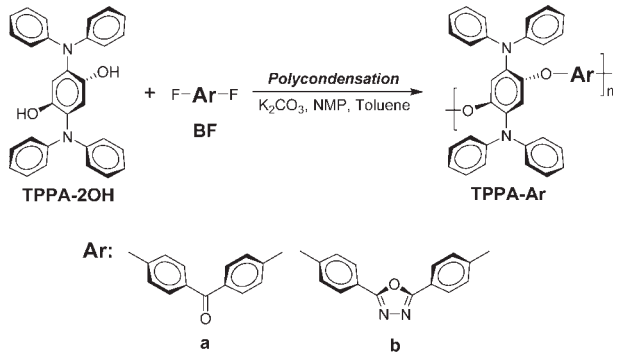

Scheme 1. Synthesis of aromatic polyethers.

Preparation of the Polyether Films

A solution of polymer was made by dissolving the polyether sample in NMP. The homogeneous solution was poured into a glass Petri dish, which was placed in a 90 °C oven for 5 h to remove most of the solvent; then the semidried film was further dried *in vacuo* at 180 °C for 8 h. The obtained films were used for solubility tests and thermal analyses.

MEASUREMENTS

Elemental analyses were run in a Heraeus VarioEL-III CHNS elemental analyzer. The inherent viscosities were determined at 0.5 g/dL concentration using Tamson TV-2000 viscometer at 30 °C. Gel permeation chromatographic (GPC) analysis was performed on a Lab Alliance RI2000 instrument (one column, MIXED-D from Polymer Laboratories) connected with one refractive index detector from Schambeck SFD Gmbh. All GPC analyses were performed using a polymer/DMF solution at a flow rate of 1 mL/min at 70 °C and calibrated with polystyrene standards. Thermogravimetric analysis (TGA) was conducted with a PerkinElmer Pyris 1 TGA. Experiments were carried out on ~6–8 mg film samples heated in flowing nitrogen or air (flow rate = 20 cm^3/min) at a heating rate of 20 °C/min. The DSC analyses were performed on a PerkinElmer Pyris Diamond DSC at a scan rate of 20 °C/min in flowing nitrogen (20 cm^3/min). Softening temperatures (T_s) were taken as the onset temperatures of probe displacement on the TMA traces. Electrochemistry was performed with a CH Instruments 611B electrochemical analyzer. Voltammograms are presented with the positive potential pointing to the left and with increasing anodic currents pointing downward. Cyclic voltammetry (CV) was conducted with the use of a three-electrode cell in which indium-tin oxide (ITO) (polymer films area about 0.5 × 1.6 cm) was used as a working electrode. A platinum wire was used as an auxiliary electrode. All cell potentials were taken by using a homemade Ag/AgCl, KCl (sat.) reference electrode. Spectroelectrochemical experiments were carried out in a cell built from a 1 cm commercial UV-visible cuvette using Hewlett-Packard 8453 UV-Visible diode array spectrophotometer. The ITO-coated glass slide was used as the working electrode, a platinum wire as the counter electrode, and a Ag/AgCl cell as the reference electrode. CE (η) determines the amount of optical density change (δOD) at a specific absorption wavelength induced as a function of the injected/ejected charge (Q; also termed as electroactivity) which is determined from the *in situ* experiments. CE is given by the equation: $\eta = \delta OD/Q = \log[T_b/T_c]/Q$, where η (cm^2/C) is the CE at a given wavelength, and T_b and T_c are the bleached and colored transmittance values, respectively. The thickness of the polyether thin films was measured by α-step profilometer (Kosaka Lab., Surfcorder ET3000, Japan). Colorimetry measurements were obtained using a Minolta CS-100A Chroma Meter. The color coordinates are expressed in the CIE 1931 Yxy color spaces.

Table 1. Inherent Viscosity,[a] Molecular Weights,[b] and Solubility Behavior of Polyethers

				Solubility in Various Solvent[d]						
Polymer	η_{inh} (dL/g)	M_w	PDI[c]	NMP	DMAc	DMF	THF	$CHCl_3$	Toluene	CH_3CN
TPPA-a	0.36	57,000	1.90	++	++	++	++	++	++	−
TPPA-b	0.42	25,000	1.39	+	+	+	+−	+	+−	−

[a] Measured at a polymer concentration of 0.5 g/dL in NMP at 30 °C.
[b] Calibrated with polystyrene standards, using DMF as the eluent at a constant flow rate of 1 mL/min at 70 °C.
[c] Degree of Polymerization.
[d] The solubility was determined with a 1 mg sample in 1 mL of a solvent. ++, soluble at room temperature; +, soluble on heating; +−, partially soluble or swelling; −, insoluble even on heating.

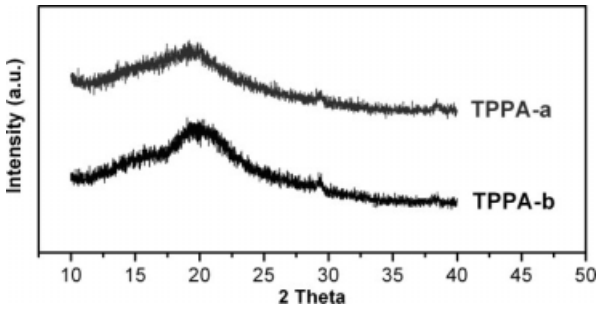

Figure 1. XRD pattern of poly(aryl-ether)s films.

RESULTS AND DISCUSSION

Polymer Synthesis

A series of newly TPPA-based poly(aryl-ether)s were synthesized from the biphenol monomer **TPPA-2OH** with corresponding difluoro compounds **BF**s (Scheme 1). The polymerization was carried out via potassium carbonate-mediated high temperature solution polycondensation. All polymerization reactions proceeded homogenously and gave high molecular weights. The obtained polyethers had inherent viscosities in the range of 0.36–0.42 dL/g with weight-average molecular weights (M_w) and polydispersity index ranged of 25,000–57,000 Da and 1.39–1.90, respectively, relative to polystyrene standards (Table 1).

Polymer Properties

Basic Characterization

The solubility properties of the polyethers were investigated qualitatively, and the results are also listed in Table 1. The polyether **TPPA-a** with benzophenone groups in the polymer main chain showed higher solubility than **TPPA-b** with coplanar oxadiazole groups in polar aprotic organic solvents such as NMP, *N,N*-dimethylacetamide, *N,N*-dimethylformamide (DMF), and toluene. The wide-angle X-ray diffraction diagram studies (shown in Fig. 1) of these polyether films revealed amorphous nature, which also reflected in their good solubility. Thus, the result good solubility makes these polymers as potential candidates for practical applications by spin-coating or inkjet-printing processes to afford high performance thin films for optoelectronic devices.

The thermal properties of polyethers were examined by TGA, TMA, and DSC, and the thermal behavior data were summarized in Table 2. Typical TGA and TMA curves of representative polyether **TPPA-a** were shown in Figure 2. All the prepared polyethers exhibited good thermal stability with insignificant weight loss up to 400 °C under nitrogen or air atmosphere. The 10% weight loss temperatures of these polymers in nitrogen and air were recorded in the range of 520–530 °C and 520–530 °C, respectively. The concentration of carbonized residue (char yield) of these polymers in a nitrogen atmosphere was more than 40% at 800 °C. The high char yields of these polymers can be ascribed to their high aromatic content. The glass-transition temperatures (T_g) of polyethers could be easily measured in the DSC thermograms; they were observed in the range of 182–205 °C, depending upon the stiffness of the polymer chain. All the polymers indicated no clear melting endotherms up to the decomposition temperatures on the DSC thermograms, which supports the amorphous nature of these polyethers. The softening temperatures (T_s) (may be referred as apparent T_g) of the polymer film samples were determined by the TMA method

Table 2. Thermal Properties of Polyethers

			T_d^5 (°C)[d]		T_d^{10} (°C)[d]		
Polymer[a]	T_g (°C)[b]	T_s (°C)[c]	N_2	Air	N_2	Air	R_{w800} (%)[e]
TPPA-a	182	182	505	505	530	530	53
TPPA-b	205	195	500	495	520	520	40

[a] The polymer film samples were heated at 200 °C for 1 h prior to all the thermal analyses.
[b] Midpoint temperature of baseline shift on the second DSC heating trace (rate: 20 °C/min) of the sample after quenching from 400 °C to 50 °C (rate: 200 °C/min) in nitrogen.
[c] Softening temperature measured by TMA with a constant applied load of 10 mN at a heating rate of 10 °C/min.
[d] Temperature at which 5% and 10% weight loss occurred, respectively, recorded by TGA at a heating rate of 20 °C/min and a gas flow rate of 30 cm^3/min.
[e] Residual weight percentages at 800 °C under nitrogen flow.

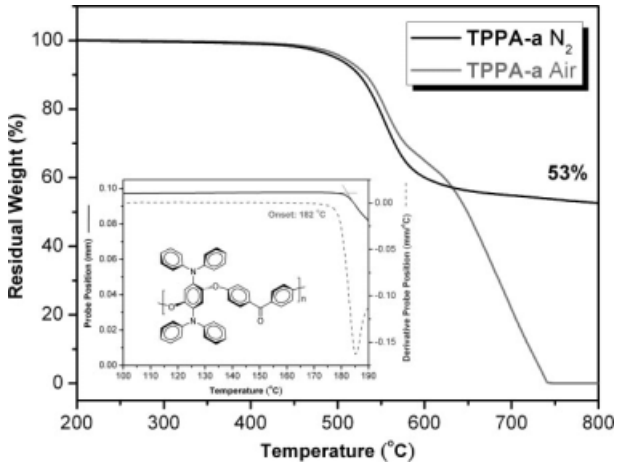

Figure 2. TGA and TMA curves of polyether **TPPA-a**.

with a loaded penetration probe. They were obtained from the onset temperature of the probe displacement on the TMA traces. In most cases, the T_s values obtained by TMA are comparable with the T_g values measured by the DSC experiments.

Electrochemical Properties

The electrochemical properties of the polyethers were investigated by CV conducted for the cast film on an ITO-coated glass substrate as working electrode in anhydrous CH_3CN and DMF containing 0.1 M of TBAP as an electrolyte under nitrogen atmosphere for oxidation and reduction measurements, respectively. Figure 3 displays the typical CV curves of TPPA-based polyethers which undergoes two reversible oxidation and one reduction processes. As shown in Table 3, the reduction behavior of polyethers **TPPA-a** and **TPPA-b** were attributed the methanone and oxadiazole groups in the polymer main chain, respectively. During the electrochemical oxidation scanning of the polyether thin films, the color of the film changed from colorless to yellow, green, and then to blue. The redox potentials of the polyethers and their respective highest occupied molecular orbital and lowest unoccupied molecular orbital (on the basis that ferrocene/ferrocenium is 4.8 eV below the vacuum level with $E_{onset} = 0.36$ V) estimated from the onset of their oxidation or reduction in CV experiments are summarized in Table 3.[13]

Spectroelectrochemical and Electrochromic Properties

Spectroelectrochemical experiments were used to evaluate the optical properties of the electrochromic films. For the investigations, the polyether film was cast on an ITO-coated glass slide, and a homemade electrochemical cell was built from a commercial ultraviolet (UV)-visible cuvette. The cell was placed in the optical path of the sample light beam in a UV-vis-NIR spectrophotometer, which allowed us to acquire electronic absorption spectra under potential control in a 0.1 M TBAP/MeCN solution. The UV-vis-NIR absorbance curves of **TPPA-a** film correlated to applied potentials are depicted in Figure 4, and the three-dimensional transmittance-wavelength-applied potential correlation of this sample is revealed in Figure 5. The **TPPA-a** film exhibited strong absorption at around 313 nm, characteristic for

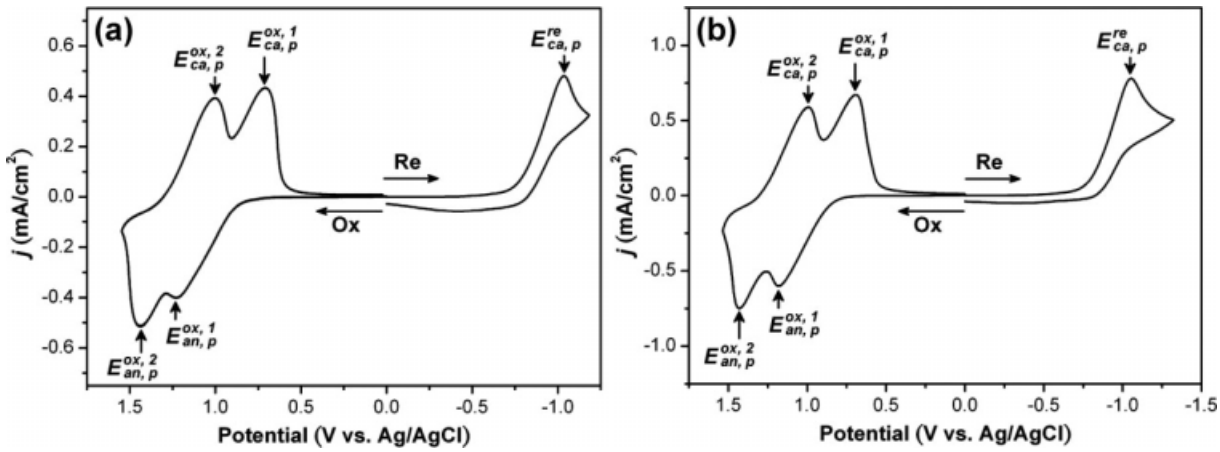

Figure 3. Cyclic voltammogram of (a) **TPPA-a** and (b) **TPPA-b** films on ITO-coated glass substrate in CH_3CN (oxidation) and DMF (reduction) solutions containing 0.1 M TBAP at scan rate of 100 mV/s.

Table 3. Redox Potentials and Energy Levels of Polyethers

	Oxidation/V[a]			Reduction/V[b]			
	$E_{1/2}$						
Index	1st	2nd	E_{onset}	E_{onset}	E_{HOMO} (eV)[c]	E_{LUMO} (eV)[c]	E_g (eV)[d]
TPPA-a	0.97	1.22	0.86	−0.78	5.30	3.66	1.64
TPPA-b	0.94	1.21	0.85	−0.78	5.29	3.66	1.63

[a] From cyclic votammograms vs. Ag/AgCl in CH_3CN. $E_{1/2}$: Average potential of the redox couple peaks.
[b] From cyclic votammograms vs. Ag/AgCl in DMF.
[c] The energy levels were calculated from cyclic voltammetry and were referenced to ferrocene (4.8 eV; onset = 0.36 V).
[d] Difference between E_{HOMO} and E_{LUMO}.

TPA unit in the neutral form (0 V), with almost colorless and transparent in the visible region. Upon oxidation (increasing applied voltage from 0 to 1.30 V), the intensity of the absorption peak at 313 nm gradually decreased whereas a new peak at 423 nm and a broad band having its maximum absorption wavelength at 1080 nm in the NIR region gradually increased in intensity. We attribute the spectral change in visible range to the formation of a stable monocation radical of the TPA unit in TPPA moiety. Furthermore, the broad absorption in NIR region was the characteristic result because of IV-CT excitation associated with ET from active neutral nitrogen atom to the cation radical nitrogen center of TPPA moiety, which was consistent with the phenomenon classified by Robin and Day.[6] As the anodic potential increasing to 1.50 V, the absorption bands of the cation radical decreased gradually with a new broad band centered around 660 nm. The disappearance of NIR absorption band can be attributable to the further oxidation of monocation radical species to the formation of dication in the TPPA segments. From the inset shown in Figure 4, the polyether **TPPA-a** film switches from a transmissive neutral state (colorless; Y: 85; *x*, 0.310; *y*, 0.332) to a highly absorbing semioxidized state (yellow; Y: 40; *x*, 0.403; *y*, 0.482), (green; Y: 20; *x*, 0.294; *y*, 0.408), and a fully oxidized state (blue; Y; 7; *x*, 0.264; *y*, 0.289). The distribution of coloration across the polymer film was very homogeneous and still

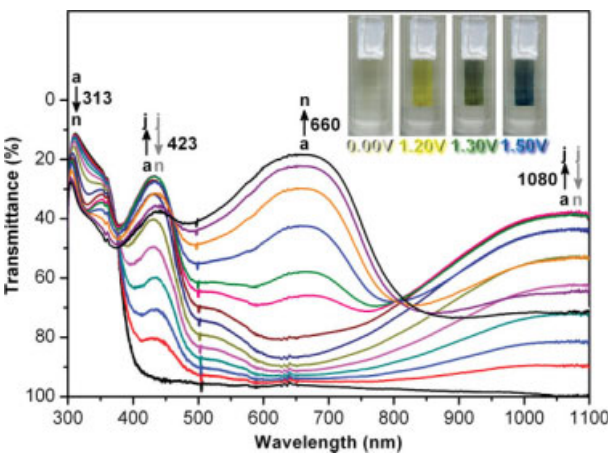

Figure 4. Electrochromic behavior of polyether **TPPA-a** thin film (~80 nm in thickness) on the ITO-coated glass substrate in 0.1 M TBAP/CH_3CN at applied potentials of (a) 0, (b) 0.90, (c) 0.95, (d) 1.00, (e) 1.05, (f) 1.10, (g) 1.15, (h) 1.20, (i) 1.25, (j) 1.30, (k) 1.35, (l) 1.40, (m) 1.45, (n) 1.50 (V vs. Ag/AgCl).

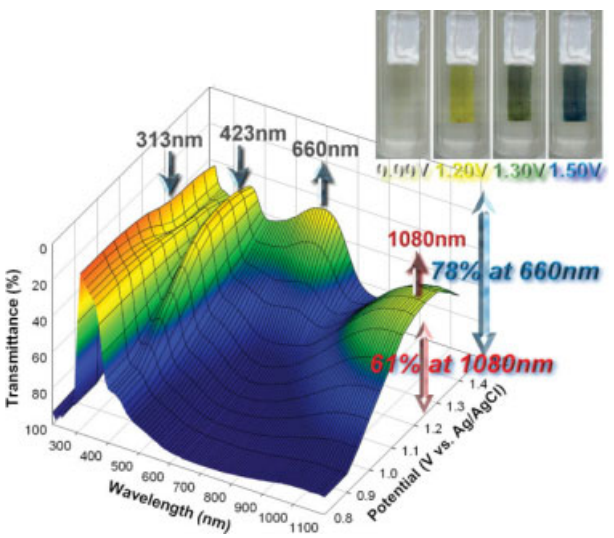

Figure 5. 3-D spectroelectrochemical behavior of the **TPPA-a** thin film on the ITO-coated glass substrate in 0.1 M TBAP/CH_3CN from 0.8 to 1.50 V (vs. Ag/AgCl).

stable even after more than hundreds of redox cycles. The polymer **TPPA-a** shows good contrast both in the visible and NIR regions with an extremely high optical transmittance change ($\Delta\%T$) of 70% at 423 nm and 61% at 1080 nm for green coloring and 78% at 660 nm for blue coloring, respectively.

For electrochromic switching studies, polymer films were cast on ITO-coated glass slides in the same manner as described earlier, and chronoamperometric and absorbance measurements were performed. Although the films were switched, the absorbance at the given wavelength was monitored as a function of time with UV-vis-NIR spectroscopy. The switching time of polyether **TPPA-a** shown in Figure 6 was calculated at 90% of the full switch because it is difficult to perceive any further color change with naked eye beyond this point. As depicted in Figure 6(a), polyether **TPPA-a** thin film revealed switching time of 3.76 s at 1.10 V for coloring process at 423 nm and 0.97 s for bleaching. The amounts of Q were calculated by integration of the current density and time obtained from Figure 6(b) as 2.677 and 2.434 mC/cm^2 for oxidation and reduction process at the first oxidation stage, respectively. The ratio of the charge density was 90.9%, indicated that charge injection/extraction was reversible during the electrochemical reactions. The electrochromic stability of the polyether **TPPA-a** film was determined by measuring the optical change as a function of the number of switching cycles shown in Figure 7. The electrochromic CE ($\eta = \delta OD/Q$) and injected charge (electroactivity) after various switching steps are summarized in Table 4. The electrochromic behavior of **TPPA-a** film exhibited high CE up to 217 cm^2/C at 423 nm within 1.4% of CE loss after switching 100 times between 0 and 1.10 V, and retained 95% of their electroactivity even after further 500 switching cycles.

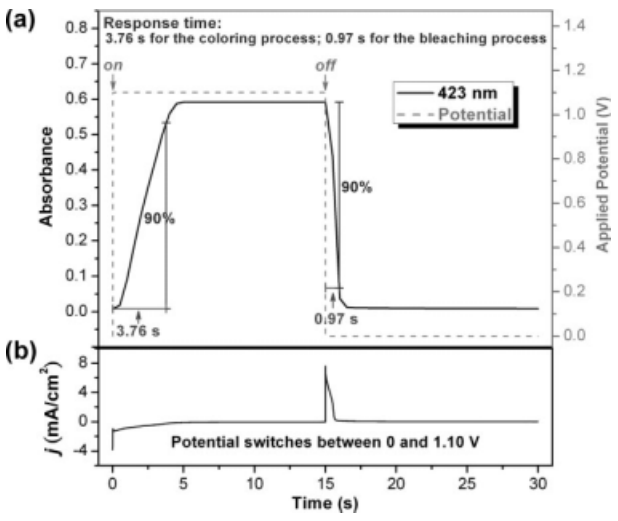

Figure 6. Calculation of optical switching time at (a) 423 nm at the applied potential and (b) current-time curves of polyether **TPPA-a** thin film (~80 nm in thickness) on the ITO-coated glass substrate (coated area: 1.6 × 0.5 cm) in 0.1 M TBAP/CH_3CN.

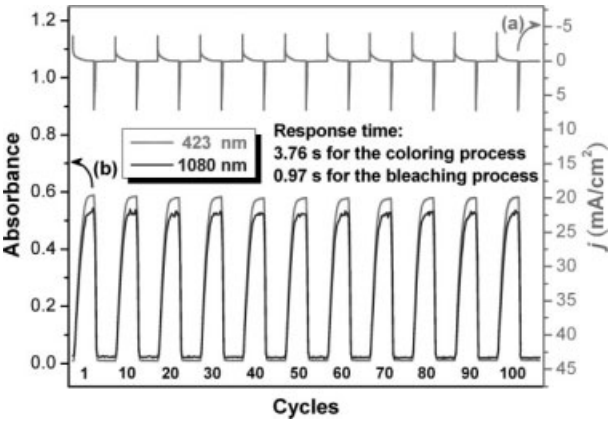

Figure 7. (a) Current consumption and (b) electrochromic switching between 0 and 1.10 V (vs. Ag/AgCl) and absorbance change monitored at 423 nm and 1080 nm of polyether **TPPA-a** thin film (~80 nm in thickness) on the ITO-coated glass substrate (coated area: 1.6 × 0.5 cm) in 0.1 M TBAP/CH_3CN with a cycle time of 20 s.

Table 4. Optical and Electrochemical Data Collected for Coloration Efficiency Measurements of Polyether **TPPA-a**

Cycling Times[a]	δOD_{423}[b]	Q (mC/cm^2)[c]	η (cm^2/C)[d]	Decay (%)[e]
1	0.580	2.677	217	0
10	0.580	2.677	217	0
20	0.579	2.677	216	0.46
30	0.578	2.676	216	0.46
40	0.577	2.676	216	0.46
50	0.576	2.675	215	0.92
60	0.575	2.675	215	0.92
70	0.574	2.674	215	0.92
80	0.574	2.673	215	0.92
90	0.572	2.673	214	1.38
100	0.571	2.673	214	1.38

[a] Switching between 0.00 and 1.10 (V vs. Ag/AgCl).
[b] Optical density change at 423 nm.
[c] Ejected charge, determined from the *in situ* experiments.
[d] Coloration efficiency is derived from the equation: $\eta = \delta OD_{423}/Q$.
[e] Decay of coloration efficiency after cyclic scans.

CONCLUSIONS

A series of NIR electroactive poly(aryl-ether)s were synthesized from the diol monomer **TPPA-2OH** with corresponding difluoro compounds **BF**s. The polymerization was carried out via potassium carbonate-mediated high temperature solution polycondensation. Introduction of electron-donating TPPA group to the polymer main chain not only afford high T_g and good thermal stability but also leads to good solubility of the polyethers. All the obtained polymers reveal valuable electrochromic characteristics such as high contrast both in visible range and NIR region, low switching times, good CE, and high-level electrochromic/electroactive reversibility.

The authors are grateful to the National Science Council of the Republic of China for its financial support of this work.

REFERENCES AND NOTES

1. (a) Monk, P. M. S.; Mortimer, R. J.; Rosseinsky, D. R. Electrochromism: Fundamentals and Applications, Wiley-VCH: Weinheim, Germany, 1995; (b) Mortimer, R. J. Chem Soc Rev 1997, 26, 147–156; (c) Rosseinsky, D. R.; Mortimer, R. J. Adv Mater 2001, 13, 783–793; (d) Somani, P. R.; Radhakrishnan, S. Mater Chem Phys 2003, 77, 117–133; (e) Liu, S.; Kurth, D. G.; Mohwald, H.; Volkmer, D. Adv Mater 2002, 14, 225–228; (f) Zhang, T.; Liu, S.; Kurth, D. G.; Faul, C. F. J. Adv Funct Mater 2009, 19, 642–652; (g) Maier, A.; Rabindranath, A. R.; Tieke, B. Adv Mater 2009, 21, 959–963; (h) Motiei, L.; Lahav, M.; Freeman, D.; van der Boom, M. E. J Am Chem Soc 2009, 131, 3468–3469.
2. (a) Rose, T. L.; D'Antonio, S.; Jillson, M. H.; Kon, A. B.; Suresh, R.; Wang, F. Synth Met 1997, 85, 1439–1440; (b) Franke, E. B.; Trimble, C. L.; Hale, J. S.; Schubert, M.; Woollam, J. A. J Appl Phys 2000, 88, 5777–5784; (c) Topart, P.; Hourquebie, P. Thin Solid Films 1999, 352, 243–248.
3. (a) Vickers, S. J.; Ward, M. D. Electrochem Commun 2005, 7, 389–393; (b) Schwab, P. F. H.; Diegoli, S.; Biancardo, M.; Bignozzi, C. A. Inorg Chem 2003, 42, 6613–6615; (c) Wang, S.; Todd, E. K.; Birau, M.; Zhang, J.; Wan, X.; Wang, Z. Y. Chem Mater 2005, 17, 6388–6394; (d) Qiao, W.; Zheng, J.; Wang, Y.; Zheng, Y.; Song, N.; Wan, X.; Wang, Z. Y. Org Lett 2008, 10, 641–644; (e) Qi, Y.; Wang, Z. Y. Macromolecules 2003, 36, 3146–3151.
4. (a) Sankaran, B.; Reynolds, J. R. Macromolecules 1997, 30, 2582–2588; (b) Sonmez, G.; Meng, H.; Zhang, Q.; Wudl, F. Adv Funct Mater 2003, 13, 726–731; (c) Sonmez, G.; Meng, H.; Wudl, F. Chem Mater 2004, 16, 574–580; (d) Dyer, A. L.; Grenier, C. R. G.; Reynolds, J. R. Adv Funct Mater 2007, 17, 1480–1486; (e) Li, M.; Patra, A.; Sheynin, Y.; Bendikov M. Adv Mater 2009, 21, 1707–1711.
5. (a) Creutz, C.; Taube, H. J Am Chem Soc 1973, 95, 1086–1094; (b) Lambert, C.; Noll, G. J Am Chem Soc 1999, 121, 8434–8442.
6. Robin, M.; Day, P. Adv Inorg Radiochem 1967, 10, 247–422.
7. Szeghalmi, A. V.; Erdmann, M.; Engel, V.; Schmitt, M.; Amthor, S.; Kriegisch, V.; Noll, G.; Stahl, R.; Lambert, C.; Leusser, D.; Stalke, D.; Zabel, M.; Popp, J. J Am Chem Soc 2004, 126, 7834–7845.
8. (a) Cheng, S. H.; Hsiao S. H.; Su, T. H.; Liou, G. S. Macromolecules 2005, 38, 307–316; (b) Liou, G. S.; Hsiao, S. H.; Su, T. X. J Mater Chem 2005, 15, 1812–1820; (c) Liou, G. S.; Yang, Y. L.; Oliver Su, Y. L. J Polym Sci Part A: Polym Chem 2006, 44, 2587–2603; (d) Liou, G. S.; Hsiao, S. H.; Chen, H. W. J Mater Chem 2006, 16, 1831–1842; (e) Liou, G. S.; Hsiao, S. H.; Huang, N. K.; Yang, Y. L. Macromolecules 2006, 39, 5337–5346; (f) Liou, G. S.; Chen, H. W.; Yen, H. J. J Polym Sci Part A: Polym Chem 2006, 44, 4108–4121; (g) Liou, G. S.; Chen, H. W.; Yen, H. J. Macromol Chem Phys 2006, 207, 1589–1598; (h) Liou, G. S.; Chang, C. W.; Huang, H. M.; Hsiao, S. H. J Polym Sci Part A: Polym Chem 2007, 45, 2004–2014; (i) Chang, C. W.; Liou, G. S.; Hsiao, S. H. J Mater Chem 2007, 17, 1007–1015; (j) Liou, G. S.; Chang, C. W. Macromolecules 2008, 41, 1667–1674; (k) Hsiao, S. H.; Liou, G. S.; Kung, Y. C.; Yen, H. J. Macromolecules 2008, 41, 2800–2808; (l) Chang, C. W.; Chung, C. H.; Liou, G. S. Macromolecules 2008, 41, 8441–8451; (m) Chang, C. W.; Liou, G. S. J Mater Chem 2008, 18, 5638–5646; (n) Chang, C. W.; Yen, H. J.; Huang, K. Y.; Yeh, J. M.; Liou, G. S. J Polym Sci Part A: Polym Chem 2008, 46, 7937–7949.
9. (a) Liou, G. S.; Hsiao, S. H.; Chen, W. C.; Yen, H. J. Macromolecules 2006, 39, 6036–6045; (b) Liou, G. S.; Yen, H. J. J Polym Sci Part A: Polym Chem 2006, 44, 6094–6102; (c) Yen, H. J.; Liou, G. S. J Polym Sci Part A: Polym Chem 2009, 47, 1584–1594.
10. Wang, K. L.; Tseng, T. Y.; Tsai, H. L.; Wu, S. C. J Polym Sci Part A: Polym Chem 2008, 46, 6861–6871.
11. Li, H.; Hu, Y.; Zhang, Y.; Ma, D., Wang, L.; Jing, X.; Wang, F. Chem Mater 2002, 14, 4484–4486.
12. Hedrick, J. L.; Twieg, R. Macromolecules 1992, 25, 2021–2025.
13. Lee, C. C.; Yeh, K. M.; Chen, Y. J Polym Sci Part A: Polym Chem 2008, 46, 7960–7971.